THE JOURNAL OF PHYSICAL CHEMISTRY A

Article

pubs.acs.org/JPCA

A Combined Crossed Beam and Ab Initio Investigation of the Gas Phase Reaction of Dicarbon Molecules (C_2; $X^1\Sigma_g^+/a^3\Pi_u$) with Propene (C_3H_6; X^1A'): Identification of the Resonantly Stabilized Free Radicals 1- and 3-Vinylpropargyl

Beni B. Dangi, Surajit Maity, and Ralf I. Kaiser*

Department of Chemistry, University of Hawai'i at Manoa, Honolulu, Hawaii 96822, United States

Alexander M. Mebel*

Department of Chemistry and Biochemistry, Florida International University, Miami, Florida 33199, United States

Supporting Information

ABSTRACT: The crossed molecular beam reactions of dicarbon, $C_2(X^1\Sigma_g^+, a^3\Pi_u)$, with propene ($C_3H_6$; X^1A') and with the partially deuterated D3 counterparts (CD_3CHCH_2, CH_3CDCD_2) were conducted at collision energies of about 21 kJ mol^{-1} under single collision conditions. The experimental data were combined with ab initio and statistical (RRKM) calculations to reveal the underlying reaction mechanisms. Both on the singlet and triplet surfaces, the reactions involve indirect scattering dynamics and are initiated by the addition of the dicarbon reactant to the carbon−carbon double bond of propene. These initial addition complexes rearrange via multiple isomerization steps leading ultimately via atomic hydrogen elimination from the former *methyl* and *vinyl* groups to the formation of 1-vinylpropargyl and 3-vinylpropargyl. Both triplet and singlet methylbutatriene species were identified as important reaction intermediates. On the singlet surface, the unimolecular decomposition of the reaction intermediates was found to be barrier-less, whereas on the triplet surface, tight exit transition states were involved. In combustion flames, both radicals can undergo a hydrogen-atom assisted isomerization leading ultimately to the thermodynamically most stable cyclopentadienyl isomer. Alternatively, in a third body process, a subsequent reaction of 1-vinylpropargyl or 3-vinylpropargyl radicals with the propargyl radical might yield to the formation of styrene ($C_6H_5C_2H_3$) in *an entrance barrier-less* reaction under combustion-like conditions. This presents a strong alternative to the formation of styrene via the reaction of phenyl radicals with ethylene, which is affiliated with an entrance barrier of about 10 kJ mol^{-1}.

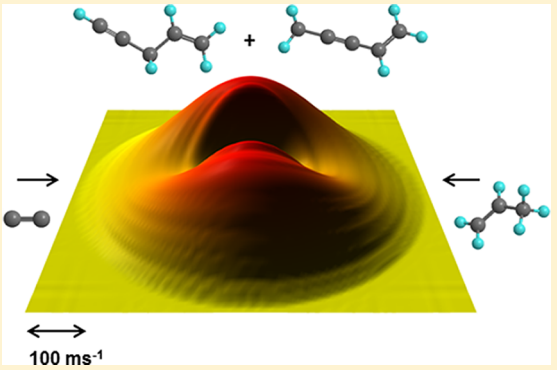

1. INTRODUCTION

Polycyclic aromatic hydrocarbons (PAHs), such as pyrene, benz[a]anthracene, and benzo[k]fluoranthene, are toxic by-products formed during the incomplete combustion of fossil and bio fuels and are considered potent atmospheric pollutants due to their carcinogenic and mutagenic characters.[1−3] The formation mechanisms of these polycyclic aromatic hydrocarbons are of particular interest to the combustion and astronomical communities due to the critical role of PAHs as reaction intermediates in soot growth[4] and also in the formation of nanometer sized carbonaceous dust particles in the outflow of circumstellar envelopes such as of IRC+10216.[5] In combustion systems, sophisticated flame tests have been the most popular investigatory technique designed to model conditions in internal combustion engines.[6−10] These studies utilize mass spectrometry often coupled with single photon (soft) photoionization to determine the nature of the isomeric species in laminar premixed low pressure flames consisting of the hydrocarbon fuel mixed with oxygen and argon.[9,11,12] Chemical kinetic models of those flame results are exploited to suggest likely reaction mechanisms of how PAHs and ultimately soot might be formed. Mass growth processes are believed to start at the molecular level and reach particulate size up to a few nanometers,[9,11,13,14] with the synthesis of the very first mono cyclic structures such as the phenyl radical (C_6H_5) and benzene (C_6H_6) suggested to be the rate-determining step.[15,16]

These studies suggest further that the chemical evolution of macroscopic environments such as combustion flames and the

Special Issue: Curt Wittig Festschrift

Received: March 18, 2013
Revised: May 15, 2013
Published: May 17, 2013

   dx.doi.org/10.1021/jp402700j | J. Phys. Chem. A 2013, 117, 11783−11793

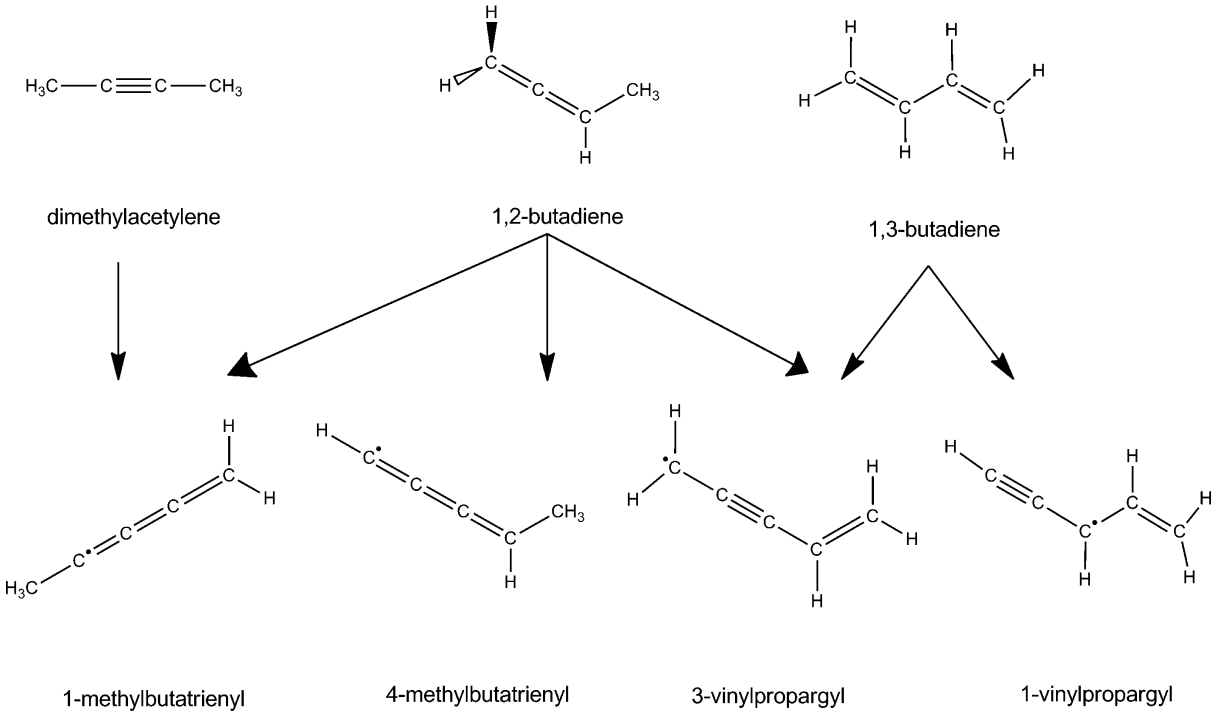

Figure 1. Distinct C_5H_5 isomers (bottom) formed via atomic hydrogen loss in the reactions of atomic carbon with distinct C_4H_6 isomers (top).

interstellar medium and the inherent formation of PAHs and dust can be best understood in terms of successive bimolecular reactions[6,9,10,17−21] often involving resonantly stabilized free radicals (RSFRs) and aromatic radicals (ARs).[4−14,22] In RSFRs such as propargyl (C_3H_3; X^2B_1),[23−26] 1,2,3-butatrien-1-yl (i-C_4H_3; X^2A'),[12,27,28] and cyclopentadienyl (C_5H_5; X^2E_1''),[12,27−30] the unpaired electron is delocalized and spread out over two or more sites in the molecule. This results in a number of resonant electronic structures of comparable importance. Owing to the delocalization, resonantly stabilized free hydrocarbon radicals are, similar to ARs such as phenyl (C_6H_5; X^2A_1),[6] more stable than ordinary radicals. Consequently, RSFRs and ARs can reach high concentrations in flames. These high concentrations make them important reactants to be involved in the formation of PAHs.[16,26,31,32]

Among these radicals, the C_5H_5 potential energy surface (PES), including cyclopentadienyl and its acyclic isomers,[33−35] has received considerable attention since the recombination of two cyclopentadienyl radicals (C_5H_5) and possibly the reaction of cyclopentadienyl with cyclopentadiene (C_5H_6) might eventually produce naphthalene and indene.[30,36,37] The formation of PAH containing five- and six-member rings is of particular interest[29,38,39] since these compounds play an important role in reaction mechanisms governing the mass growth of higher PAHs, soot, and even fullerenes[40,41] in combustion flames.[42,43] Simple PAH species with five-membered rings including indene, fluorene, 1H-benz[f]indene, and 1H-benz[e]indene, are abundant in flames and may be involved in further PAH growth producing nonplanar bowl-shaped structures, which are possible precursors of fullerenes. Indene is the simplest PAH molecule with a five-membered ring, and the chemical reactions, which can potentially lead to its formation in combustion flames, include, for instance, reactions of phenyl radicals with methylacetylene/allene.[44,45]

Sophisticated crossed molecular beam experiments combined with electronic structure calculations provided compelling evidence that distinct C_5H_5 isomers can be formed in bimolecular reactions of ground-state carbon atoms, $C(^3P_j)$, with C_4H_6 isomers 1,3-butadiene,[46] 1,2-butadiene,[47] and dimethylacetylene[48] on the triplet surface (Figure 1) via C_5H_6 intermediates. An alternative pathway to access the C_5H_6 surface ultimately leading to the formation of distinct C_5H_5 radicals via atomic hydrogen loss might be the bimolecular reactions of dicarbon molecules, C_2, in its electronic ground ($X^1\Sigma_g^+$) and first excited state ($a^3\Pi_u$) with propene (C_3H_6; X^1A'). Note that both dicarbon in its singlet ground state and in its triplet excited state as well as propene have been detected in hydrocarbon flames[49,50] and in the interstellar medium.[51,52] These reactions are expected to form hydrocarbon radicals, possibly RSFRs, via the dicarbon versus atomic hydrogen loss pathways as shown, for instance, in the bimolecular reactions of dicarbon with ethylene and acetylene yielding the 1,2,3-butatrien-1-yl (i-C_4H_3; X^2A')[53] and butadiynyl (C_4H; $X^2\Sigma^+$), respectively.[54] Previous studies on the dicarbon−propene system were limited to the investigation of the inherent kinetics.[55,56] Daugey et al. reported the kinetics utilizing a continuous supersonic flow reactor in the temperature range of 77 to 296 K, suggesting rate constants in the order of 10^{-10} cm^3 s^{-1}.[56] However, these studies could only probe the decay kinetics of the dicarbon reactant, but not the explicit formation of reaction products under single collision conditions. Therefore, here, we present results of the dicarbon−propene system under single collision conditions and compare the reaction products, mechanisms, and chemical dynamics with the $C(^3P_j)$−C_4H_6 systems probed earlier.[46−48]

2. EXPERIMENTAL METHODS

The experiments were conducted under single collision conditions utilizing a universal crossed molecular beam machine.[57,58] Briefly, a pulsed supersonic dicarbon beam, $C_2(X^1\Sigma_g^+, a^3\Pi_u)$, was generated by laser ablation of graphite at 266 nm. The rotating and translating graphite rod was

dx.doi.org/10.1021/jp402700j | J. Phys. Chem. A 2013, 117, 11783−11793

ablated by focusing 10−15 mJ per pulse of the output of a Spectra-Physics Quanta-Ray Pro 270 Nd:YAG laser operating at 30 Hz and seeding the ablated species in neon carrier gas (99.9999%, Specialty Gases). The latter was introduced via a Proch-Trickl pulsed valve operating at repetition rates of 60 Hz with amplitudes of −350 V to −400 V and opening times of 80 μs. A neon gas backing pressure of 4 atm resulted in a pressure of about 4×10^{-4} Torr in the primary source chamber. The molecular beam passed a skimmer and a four-slot chopper wheel, which selected a segment of the pulsed dicarbon beam of a well-defined peak velocity (v_p) and speed ratio (S) (Table 1). The segment of the pulsed dicarbon beam then crossed a

Table 1. Peak Velocities (v_p), Speed Ratio (S), Collision Energy (E_c), and Center-of-Mass Angles (Θ_{CM}) of the Dicarbon, Propene, and Partially Deuterated Propene Molecular Beams

beam	v_p (ms^{-1})	S	E_c (kJ mol^{-1})	Θ_{CM}
CH_3CHCH_2	833 ± 15	11.0 ± 0.3		
C_2	1440 ± 32	2.7 ± 0.7	21.1 ± 0.8	45.4 ± 1.1
CH_3CDCD_2	815 ± 20	7.8 ± 1.0	21.4 ± 0.9	46.7 ± 1.2
CD_3CHCH_2	815 ± 20	7.8 ± 1.0	21.4 ± 0.9	46.7 ± 1.2

pulsed propene (C_3H_6, 99+%, Sigma-Aldrich) beam perpendicularly in the interaction region. The pulsed propene beam was generated by a pulsed valve operated at a backing pressure of 550 Torr and 60 Hz thus producing a pressure of about 2×10^{-4} Torr in the secondary source chamber. A photo diode mounted on top of the chopper wheel provided the time zero of the experiments. Partially deuterated isotopologues of propene, i.e., D3-propenes CD_3CHCH_2 and CH_3CDCD_2 (99+ D%, C/D/N Isotopes Inc.), were used to elucidate the position of the atomic hydrogen loss, i.e., from the methyl versus vinyl group, and, hence, to extract the nature of the product isomers formed. Note that the primary beam contains carbon atoms and tricarbon molecules as well. The tricarbon (C_3) does not interfere with the ion counts of the dicarbon−propene system. Previous test experiments showed that tricarbon reacts with propene only at collision energies larger than about 40 kJmol^{-1}, which is much higher than the present collision energy of 21 kJ mol^{-1}. Reactive scattering signal from the reaction of atomic carbon with propene does not interfere in the mass range from 65 ($C_5H_5^+$) to m/z = 63 ($C_5H_3^+$) either. However, the presence of carbon atoms does hinder the potential detection of the methyl loss pathway; please refer to section 4.1 for a full discussion. The ablation source and the relative intensities of atomic carbon, dicarbon, and tricarbon have been characterized extensively.[59]

The neutral reaction products were analyzed by a triply differentially pumped rotatable mass spectrometer operated in the time-of-flight mode. Here, the neutral products are ionized by electron impact (80 eV, 2.0 mA), pass a quadrupole mass filter, and reach a Daly type ion detector operated at −22.5 kV.[60] The quadrupole mass spectrometer (Extrel QC 150) operated at 2.1 MHz and passed ions with the desired mass-to-charge, m/z, value. The signal from the photomultiplier tube passes a discriminator (Advanced Research Instruments, Model F-100TD, 1.6 mV) and is then fed into a Stanford Research System SR430 multichannel scaler to record the time-of-flight (TOF) spectra.[57] These TOF spectra were recorded at multiple angles in the lab frame and then integrated to obtain the angular distribution of the product(s). A forward-convolution routine was used to fit the experimental data.[61,62] This iterative method initially assumes an angular flux distribution, $T(\theta)$, and the translational energy flux distribution, $P(E_T)$ in the center-of-mass system. Laboratory TOF spectra and the laboratory angular distributions (LABs) were then calculated from the $T(\theta)$ and $P(E_T)$ functions accounting for the velocity and angular spread of each beam. Best fits were obtained by iteratively refining the adjustable parameters in the center-of-mass system within the experimental error limits of such as peak velocity, speed ratio, and error bars in the LAB distribution.

The dicarbon beam was also characterized spectroscopically *in situ* via laser-induced fluorescence (LIF) to probe the ro-vibrational distribution of the singlet ($X^1\Sigma_g^+$) and triplet ($a^3\Pi_u$) states.[58,63] Briefly, rotational temperatures (T_{rot}) were measured for the first and second vibrational levels of the first excited electronic state, $a^3\Pi_u$, via the Swan band transition ($d^3\Pi_g$−$a^3\Pi_u$). The values reported for v = 0 and v = 1 were T_{rot} = 240 ± 30 K and 190 ± 30 K with fractions of 0.67 ± 0.05 in v = 0 and 0.33 ± 0.05 in v = 1. The singlet state was probed via the Mulliken excitation ($D^1\Sigma_u^+$−$X^1\Sigma_g^+$). At v = 0 at fractions of 0.83 ± 0.1, the rotational distribution was bimodal; rotational temperatures were derived to be T_{rot} = 200 K (population fraction 0.44 ± 0.05) and T_{rot} = 1000 K (population fraction 0.39 ± 0.05). At v = 1 at fractions of 0.17 ± 0.04, a bimodal rotational distribution was also observed giving T_{rot} = 200 K (0.06 ± 0.02) and T_{rot} = 1,000 K (0.11 ± 0.02). These results clearly show the existence of singlet as well as triplet states in our dicarbon beam.

3. COMPUTATIONAL METHODS

Geometries of various species involved in the $C_2(^1\Sigma_g^+/^3\Pi_u)$ + C_3H_6 reactions, including the reactants, C_5H_6 intermediates, transition states, and products, were optimized at the hybrid density functional B3LYP level of theory with the 6-311G(d,p) basis set.[64,65] Vibrational frequencies and zero-point vibrational energy (ZPE) were obtained using the same B3LYP/6-311G(d,p) approach. The optimized geometries of all species were then used in single-point coupled cluster CCSD(T) calculations[66−69] (restricted open-shell RHF-RCCSD(T) for open-shell species) with Dunning's correlation-consistent cc-pVDZ, cc-pVTZ, and cc-pVQZ basis sets.[70] The T1 diagnostics values for calculated species appeared not to exceed 0.02, indicating that their wave functions do not exhibit a strong multireference character, and so the CCSD(T) approach should produce reliable energetics. Note that the T1 diagnostics is a measure of the magnitude of the singlet amplitudes in the coupled-cluster expansion of the wave function.[71] The CCSD(T) total energies were extrapolated to the complete basis set (CBS) limit by fitting the following equation:[72]

$$E_{tot}(x) = E_{tot}(\infty) + Be^{-Cx}$$

where x is the cardinal number of the basis set (2, 3, and 4) and $E_{tot}(\infty)$ is the CCSD(T)/CBS total energy. On the triplet surface, the CCSD(T)/cc-pVQZ calculations were performed only for the reactants, products, and the most critical transition states; otherwise, the CBS extrapolation was carried out using the CCSD(T)/cc-pVDZ and CCSD(T)/cc-pVTZ energies only with the following expression[72]

$$E_{tot}(\infty) = (E_{tot}(cc - pVTZ) - E_{tot}(cc - pVDZ) \times 2.5^3/3.5^3)/(1 - 2.5^3/3.5^3)$$

The differences between relative energies obtained from the three- and two-point extrapolation schemes are normally small, within 1−2 kJmol^{-1}, but may reach 7 kJ mol^{-1} for some exit transition states and about 10 kJ mol^{-1} for radical products. The GAUSSIAN 09[73] and MOLPRO 2010[74] programs were used for the ab initio calculations.

Rate constants $k(E)$ were computed using RRKM theory,[75−77] where the internal energy E was taken as a sum of the energy of chemical activation in the $C_2(^1\Sigma_g^+/^3\Pi_u)$ + C_3H_6 reactions and a collision energy, assuming that a dominant fraction of the latter is converted to the internal vibrational energy. The harmonic approximation was used to calculate the total number and density of states. For the reaction channels that do not exhibit exit barriers, such as H atom eliminations from various C_5H_6 intermediates occurring by a cleavage of single C−H bonds, we applied the microcanonical variational transition state theory[77] (VTST) and computed variational transition states, so that the individual microcanonical rate constants were minimized along the reaction paths of the barrierless single-bond cleavage processes. Product branching ratios were evaluated by solving first-order kinetic equations for unimolecular reactions within the steady-state approximation, according to the kinetics schemes based on the ab initio potential energy diagrams. The rate constants for the barrierless $C_2(^1\Sigma_g^+/^3\Pi_u)$ additions to propene were not considered in the present treatment, as our main goal was to evaluate product branching ratios for various dissociation channels leading to product formation independent of the total rate constant in the entrance channel.

4. RESULTS

4.1. Laboratory Data. Reactive scattering signal from the reaction of dicarbon (C_2; 24 amu) with propene (C_3H_6; 42 amu) was observed at mass-to-charge, m/z, between 65 ($C_5H_5^+$) and m/z = 63 ($C_5H_3^+$). At all masses, the TOF spectra overlapped after scaling; this finding indicates that ions at lower mass-to-charge ratios result from dissociative ionization of the C_5H_5 neutral product in the electron impact ionizer, and that only the dicarbon versus atomic hydrogen pathway is open. Note that the signal-to-noise was better for the ions at m/z = 64 and m/z = 63; hence the signal was recorded at the ion with the best signal-to-noise, i.e., m/z = 63 (Figure 2). We also attempted to probe the methyl loss pathway at m/z = 51 ($C_4H_3^+$); a strong signal was observed at m/z = 51 and data recorded from 34° to 66° in 2.5° steps. However, fitting this data revealed that the signal largely resulted from reaction of ground state carbon atoms, which are also present in the primary beam,[59] with propene (C_3H_6) forming C_4H_5 (53 amu); the latter can undergo dissociative ionization in the electron impact ionizer. Thus, if the C_4H_3 plus CH_3 product channel is present in the title reaction, it is masked by the dissociative ionization product from the reaction of ground state carbon atoms with propene. Since the reaction dynamics of the atomic carbon−propene system were reported earlier, the reader is referred to the original literature,[78] and the successive sections only focus on the reaction of dicarbon with propene. Note that besides atomic carbon and dicarbon, the primary beam also contains tricarbon molecules. However, tricarbon does not interfere with the reactive scattering signal in the range of m/z = 65 to 63, as tricarbon does not react with unsaturated hydrocarbons at collision energies as low as 40 kJ mol^{-1}.[79] We can now integrate the TOF spectra to derive the LABs of the C_5H_5 product(s). This angular distribution is shown in Figure 3 and peaks close to the center-of-mass angle

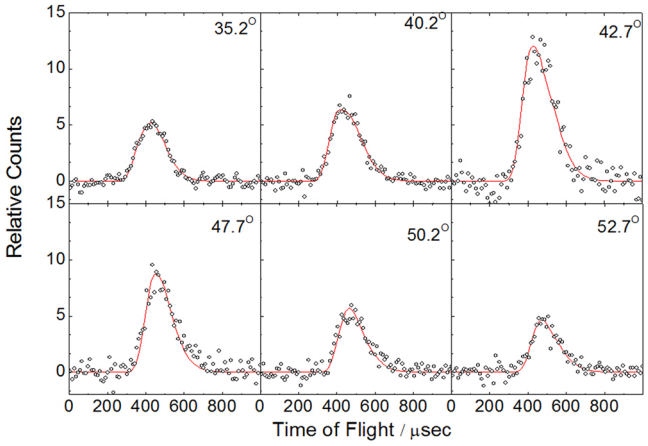

Figure 2. Time-of-flight data recorded at m/z = 63 in the reaction of dicarbon with propene at various laboratory angles at a collision energy of 21.1 kJ mol^{-1}. The circles represent the experimental data, and the solid line represents the fit.

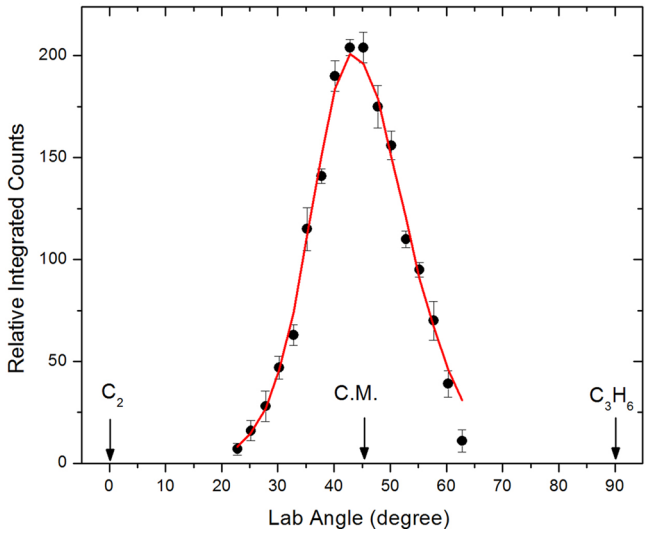

Figure 3. LAB of product signal at m/z = 63. C.M. designates the center-of-mass angle. Filled circles and 1σ error bars represent the experimental data, and the solid line represents the calculated distribution.

of 45.4° ± 1.1° (Table 1). The overall shape depicts a nearly forward−backward symmetric distribution extending at least 40° in the scattering plane defined by both beams. In summary, the interpretation of the TOF data suggests the existence of the dicarbon versus hydrogen atom exchange channel along with the formation of C_5H_5 isomer(s) at the collision energy of 21.1 ± 0.8 kJ mol^{-1} (Table 1) under single collision conditions.

Having identified the atomic hydrogen loss, it is important to elucidate whether this hydrogen atom is ejected from the vinyl or from the methyl group in propene. To determine the position of hydrogen loss, we therefore conducted experiments with partially deuterated D3-propenes (CH_3CDCD_2, CD_3CHCH_2). This also assists to determine the branching

dx.doi.org/10.1021/jp402700j | J. Phys. Chem. A 2013, 117, 11783−11793

ratio of different hydrogen loss channels and the identification of the product isomers. Here, in the reaction with CH_3CDCD_2 and CD_3CHCH_2, the hydrogen atom can be only lost from the methyl and vinyl groups, respectively. Figure 4 shows the TOF

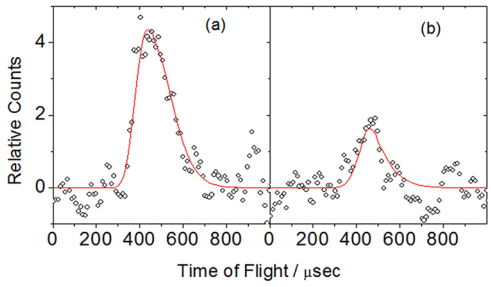

Figure 4. Time-of-flight data for the atomic hydrogen loss pathway in the reactions of dicarbon with partially deuterated propenes, (a) CH_3CDCD_2 and (b) CD_3CHCH_2 monitored at m/z = 68 ($C_5H_2D_3^+$) at the center-of-mass angle.

spectra recorded at the center-of-mass angle for CH_3CDCD_2 and CD_3CHCH_2 recorded at m/z = 68 for the atomic hydrogen loss channel ($C_5D_3H_2^+$). These raw data alone clearly indicate two distinct atomic hydrogen loss pathways from the methyl *and* from the vinyl group. Integrated signals from reactions of dicarbon with CH_3CDCD_2 and CD_3CHCH_2 indicate branching ratios of the atomic hydrogen loss from the methyl versus the vinyl position of 75 ± 10% and 25 ± 10%, respectively.

4.2. Center-of-Mass Functions. After compiling the laboratory data, we are now turning our attention to the center-of-mass functions: the translational ($P(E_T)$) and angular ($T(\theta)$) center-of-mass distributions. The laboratory data can be fit with a single channel of the mass combination of 65 amu (C_5H_5) and 1 amu (H). Figure 5 depicts the center-of-mass translational energy (top) and angular (bottom) distributions forming the C_5H_5 radical(s) and hydrogen atom. The $P(E_T)$ distribution depicts a relatively broad distribution maximum starting from zero translational energy up to 20 kJ mol^{-1}. This finding suggests that at least one reaction channel involves a tight exit transition state and hence a significant exit barrier of this order of magnitude. Second, for those products formed without internal excitation, the maximum translation energy of the $P(E_T)$ distribution, E_{max}, presents the sum of the collision energy plus the reaction exoergicity. Therefore, E_{max} can be utilized to extract the reaction energy. For the E_{max} value of 220 ± 40 kJ mol^{-1}, the reaction is determined to be exoergic by 200 ± 40 kJ mol^{-1} after subtracting the nominal collision energy. Finally, the averaged fraction of available energy released into the translational degrees of freedom of the products is approximately 29 ± 5%;[80] this fraction has been calculated for the energetics on the triplet surface and the formation of product p2. Further, the center-of-mass angular distribution is forward–backward symmetric with respect to 90° and is distributed over the complete angular range from 0° to 180°. The intensity over the complete scattering range suggests that the dicarbon–propene system involves indirect scattering dynamics via the formation of bound C_5H_6 reaction intermediate(s);[81] further, the forward–backward symmetry suggests that decomposing C_5H_6 reaction intermediate(s) is(are) long-lived, i.e., longer than the rotational period of the C_5H_6 molecule.[80] In principle, the forward–backward symmetry can also be the result of a "symmetric" reaction

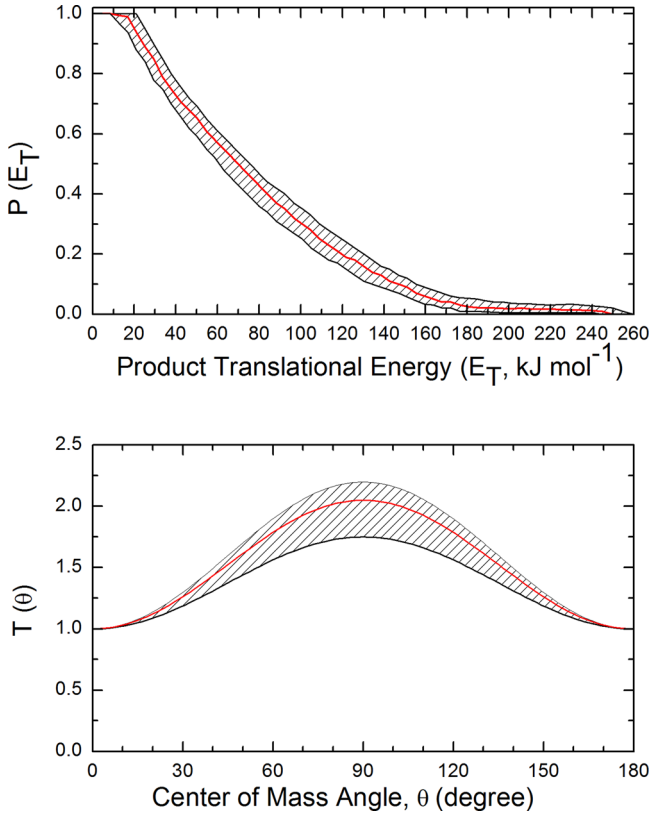

Figure 5. Center-of-mass translational energy flux distribution (upper) and angular distribution (lower) for the hydrogen atom loss channel in the dicarbon-propene reaction leading to C_5H_5 products. Hatched areas indicate the acceptable upper and lower error limits of the fits, and the solid red line defines the best-fit function.

intermediate. In the latter case, the probability of the leaving hydrogen atom from the decomposing complex is equal at θ and $\pi-\theta$. Finally, the maximum at 90° in the center-of-mass angular distribution depicts geometrical constraints of the decomposing complex ("sideways scattering"). Here, the distribution suggests that the atomic hydrogen is lost preferentially perpendicularly to the plane of the decomposing complex almost parallel to the total angular momentum vector.[80]

5. DISCUSSION

Before combining the experimental data with the computational results, let us briefly summarize the experimental results (R1–R5).

(R1) The laboratory data and TOF spectra suggest the existence of a dicarbon versus atomic hydrogen replacement mechanism leading to the formation of C_5H_5 isomer(s). The hydrogen atom can be lost from the methyl and/or vinyl group. No evidence for molecular hydrogen loss was found. A methyl elimination pathway could not be detected due to the experimental difficulties, in particular, the strong yield of the $C_4H_3^+$ product of dissociative ionization of C_4H_5, which is the primary product of the reaction of propene with carbon atoms abundant in the beam.

(R2) To elucidate whether the hydrogen atom is lost from the vinyl or from the methyl group in propene, experiments with partially deuterated D3-propenes (CH_3CDCD_2, CD_3CHCH_2) were conducted. These studies demonstrated that two distinct atomic hydrogen loss pathways from the

dx.doi.org/10.1021/jp402700j | J. Phys. Chem. A 2013, 117, 11783–11793

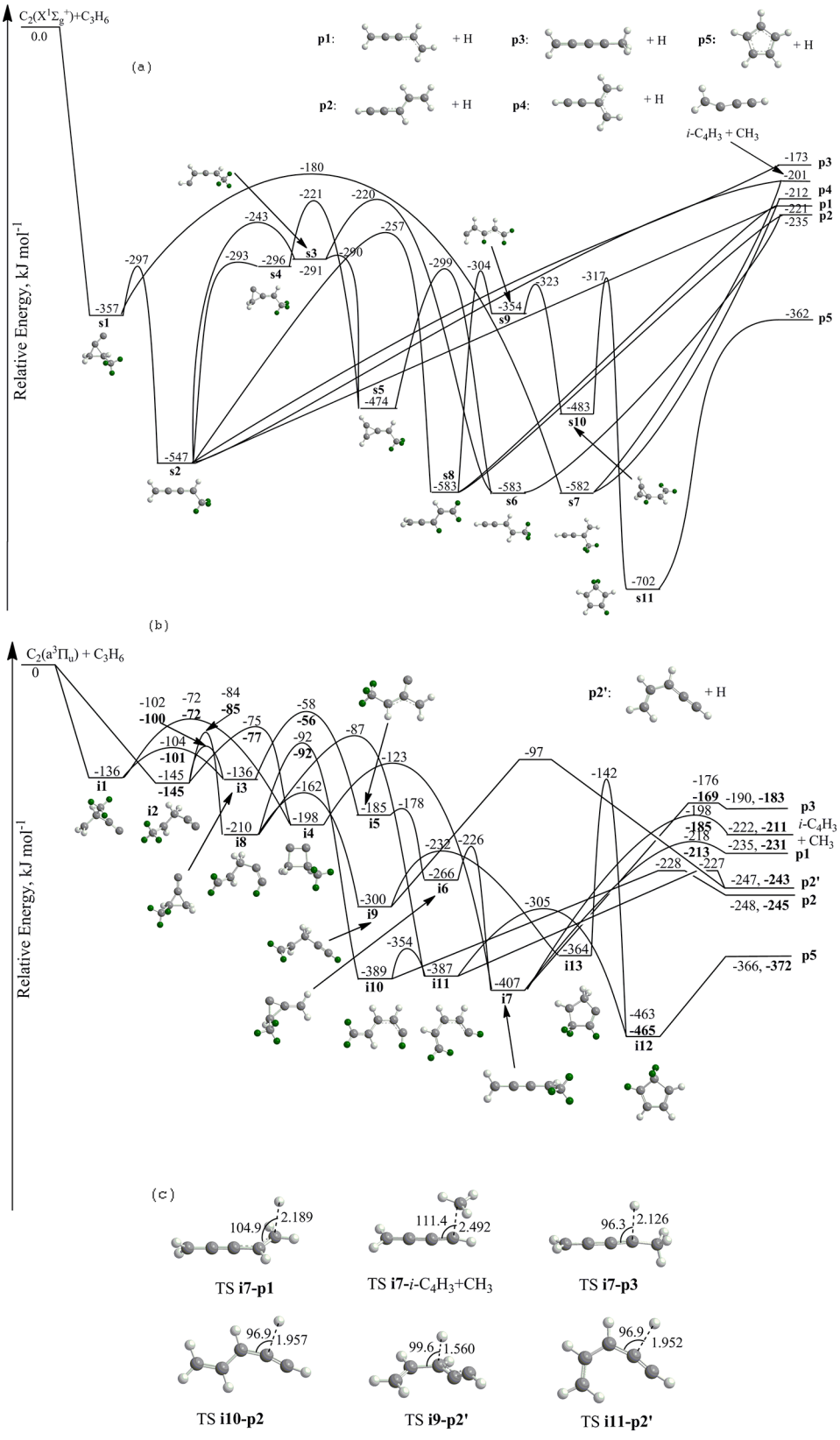

Figure 6. PESs calculated at the CCSD(T)/CBS level: (a) For the $C_2(X^1\Sigma_g^+)$ + C_3H_6 reaction, based on three-point CBS extrapolation from CCSD(T)/cc-pVDZ, CCSD(T)/cc-pVTZ, and CCSD(T)/cc-pVQZ total energies. (b) For the $C_2(a^3\Pi_u)$ + C_3H_6 reaction. Bold numbers are obtained based on the three-point CBS extrapolation and plain numbers, based on two-point CBS extrapolation from CCSD(T)/cc-pVDZ and CCSD(T)/cc-pVTZ total energies. H atoms from the methyl group are highlighted in green. Geometries of distinct exit transition states are displayed in panel c.

dx.doi.org/10.1021/jp402700j | J. Phys. Chem. A 2013, 117, 11783−11793

Table 2. Product Branching Ratios (%) in the $C_2(^1\Sigma_g^+/^3\Pi_u)$ + C_3H_6 Reaction Calculated at Various Collision Energies (kJ/mol)

(a) $C_2(^1\Sigma_g^+)$ collision energy	0.0	8.4	16.7	21.0	25.1	33.5	41.8
C_5H_5 + H $CH_2CCCHCH_2$ **p1** total	44.96	44.98	44.98	44.83	44.71	44.42	44.19
p1 from **s2**	41.20	41.33	41.41	41.31	41.22	41.01	40.89
p1 from **s8**	1.35	1.38	1.41	1.43	1.45	1.48	1.46
p1 from **s6a**	2.41	2.28	2.15	2.09	2.05	1.94	1.83
t-CHCCHCHCH2 **p2** total	13.51	13.08	12.66	12.48	12.32	12.03	11.57
p2 from **s8**	8.15	8.09	8.01	7.97	7.96	7.90	7.79
p2 from **s6**	5.36	5.00	4.65	4.51	4.36	4.14	3.78
CH_2CCCCH_3 **p3**	1.46	1.61	1.76	1.85	1.91	2.05	2.20
c-C_5H_5 **p5**	7.04	6.41	5.85	5.57	5.37	4.95	4.71
$CHCCCHCH_3$ **p6**	1.00	1.13	1.26	1.35	1.41	1.57	1.74
C_4H_3 + CH_3 *i*-C_4H_3 total	27.07	27.70	28.29	28.66	28.95	29.60	30.27
i-$C_4H_3$from **s2**	26.48	27.14	27.75	28.14	28.44	29.10	29.80
i-C_4H_3 from **s7**	0.59	0.56	0.54	0.53	0.52	0.50	0.46
n-C_4H_3	1.17	1.28	1.39	1.44	1.46	1.49	1.46
CH_3CCH + CCH_2	2.85	2.80	2.75	2.73	2.72	2.68	2.64
CH_3CCH + C_2H_2	0.73	0.77	0.80	0.83	0.84	0.89	0.89
CH_3CHCCC + H_2	0.12	0.14	0.16	0.16	0.17	0.19	0.22
CH_3CCCCH + H_2	0.09	0.09	0.10	0.10	0.10	0.11	0.11
C_4H_2 + CH_4	0.00	0.00	0.00	0.00	0.00	0.00	0.00

(b) $C_2(^3\Pi_u)$ collision energy	0.0		8.4		16.7		21.0		25.1		33.5		41.8	
from initial adduct	**i1**	**i2**	**i1**	**i2**	**i1**	**i2**	**i1**	**i2**	**i1**	**i2**	**i1**	**i2**	**i1**	**i2**
C_5H_5 + H $CH_2CCCHCH_2$ **p1**	23.64	21.62	24.14	21.86	24.39	21.87	24.51	21.87	24.59	21.83	24.66	21.69	24.73	21.55
t-$CHCCHCHCH_2$ **p2**	2.53	2.68	2.84	3.04	3.10	3.36	3.23	3.52	3.34	3.66	3.56	3.96	3.76	4.22
c-$CHCCHCHCH_2$	26.73	28.29	28.39	30.39	29.74	32.21	30.31	33.03	30.77	33.73	31.53	34.99	32.05	36.02
p2′ from **i9**	25.29	26.77	26.79	28.67	27.97	30.29	28.47	31.02	28.85	31.63	29.49	32.73	29.90	33.60
p2′ from **i11**	1.43	1.52	1.60	1.72	1.77	1.91	1.84	2.01	1.92	2.10	2.04	2.27	2.16	2.42
CH_2CCCCH_3 **p3**	1.05	0.96	1.18	1.07	1.31	1.18	1.38	1.23	1.45	1.28	1.58	1.39	1.71	1.49
c-C_5H_5 **p5**	30.10	31.85	26.05	27.88	22.64	24.52	21.06	22.95	19.71	21.61	17.20	19.09	15.10	16.97
$CHCCCHCH_3$ **p6**	1.31	1.20	1.51	1.37	1.73	1.55	1.84	1.64	1.95	1.73	2.24	1.97	2.40	2.09
i-C_4H_3 + CH_3	14.64	13.40	15.89	14.39	17.08	15.31	17.66	15.76	18.20	16.16	19.22	16.91	20.25	17.65

methyl *and* from the vinyl group exist. Branching ratios of the atomic hydrogen loss from the methyl versus the vinyl position of 75 ± 10% and 25 ± 10%, respectively, were derived.

(R3) The reaction follows indirect scattering dynamics via the involvement of C_5H_6 complexes; the latter are long-lived; at least one of the intermediates decomposes via hydrogen atom loss almost parallel to the total angular momentum vector.

(R4) The reaction forming C_5H_5 plus atomic hydrogen is exoergic by about 200 ± 40 kJ mol^{-1}.

(R5) At least one channel involves a tight exit transition state as indicative from the relatively broad distribution maximum of the center-of-mass translational energy distribution starting from zero translational energy up to 20 kJ mol^{-1}.

As evident from the complex singlet and triplet PESs (Figure 6), the dicarbon−propene reaction presents a tricky system. The calculations predict that five C_5H_5 reaction products can be formed (**p1**−**p5**). On the basis of the calculations alone, all isomers are accessible on the singlet surface, but only reaction pathways to **p1**, **p2**, **p3**, and **p5** were located on the triplet surface. Here, the cyclopentadienyl radical (**p5**) presents the thermodynamically most stable C_5H_5 structure. It is 127 and 141 kJ mol^{-1} more stable than **p2** and **p1**, respectively, which can be considered as vinyl-substituted C1 and C3 propargyl radicals. Isomer **p4**, formally an ethynyl substituted allyl radical, is 150 kJ mol^{-1} less stable than the cyclopentadienyl radial **p5**. Note that product **p3** is the energetically least stable C_5H_5 isomer among those considered here; it can be derived from the 1,2,3-butatrien-1-yl radical by replacing the C1 hydrogen atom by a methyl group. In the case of complex PESs, the very first step is to compare the experimentally derived energetics (−200 ± 40 kJ mol^{-1}) of the reaction with the calculated data of the isomers **p1** to **p5**. The energetics of the formation of the cyclopentadienyl radical **p5** do not correlate well with the experimental findings depicting deviations of about 160 kJ mol^{-1}. Therefore, we can conclude that cyclopentadienyl is likely not the reaction product. On the other hand, the experimental reaction energy can account within the error limits for the formation of any of the isomers **p1** to **p4**.

Having identified **p1** to **p4** as possible reaction products, we are attempting to narrow down the choices even further. Recall that experiments with D3-propenes (CH_3CDCD_2, CD_3CHCH_2) indicate that the hydrogen atom can be lost from the methyl group and from the vinyl group with emission from the methyl group being dominant (75 ± 10%) over the vinyl group (25 ± 10%). On the triplet surface, having eliminated **p5** as a reaction product, the computations predict **p1** as the only remaining reaction product formed via atomic hydrogen loss from the *methyl group* of the triplet 1-methylbutatriene reaction intermediate (**i7**). The latter can also fragment via hydrogen atom elimination from the "vinyl" group yielding **p3**. Finally, reaction products **p2** and **p2′**, the cis isomer of **p2**, are accessible via hydrogen atom loss from "vinyl"

dx.doi.org/10.1021/jp402700j | J. Phys. Chem. A 2013, 117, 11783−11793

hydrogen atoms of intermediates of **i10** as well as **i9** and **i11**, respectively. On the singlet surface, the situation is even more complex. A close look at the reaction pathways indicates that **p1**, **p2**, and **p4** can be synthesized via hydrogen atom emission from the former methyl group: intermediates **s2** and **s8** can fragment to **p1**, whereas **p2** and **p4** can originate from intermediate **s6** and **s7**, respectively. On the other hand, the calculations suggest **s8** and **s2** as potential intermediates in the formation of **p2** and **p3**, respectively, via hydrogen atom loss from the former vinyl group. Therefore, the calculations indicate that on the singlet *and* triplet surfaces, hydrogen atom emissions from the *methyl and vinyl* groups are energetically accessible.

These considerations suggest that on the triplet surface, **p1** represents an accessible reaction product formed via unimolecular decomposition through atomic hydrogen loss from the *methyl* group of **i7**; on the other hand, products **p2**/**p2′** as well as **p3** could originate via atomic hydrogen loss from the former *vinyl* group of intermediates **i9**-**i10** and **i7**, respectively. Considering the energetics involved in the unimolecular decomposition of intermediate **i7**, the significantly lower exit barriers (−213 versus −169 kJmol^{-1}) and favorable energetics (−231 versus −183 kJmol^{-1}) are expected to prefer the formation of **p1** compared to **p3**. This conclusion gains full support from the statistical calculations indicating that intermediate **i7** decomposes preferentially to **p1** compared to **p3** with fractions of 23% and 1% of the total product yield, respectively (Table 2 and the unimolecular decomposition rate constants of **i7** in Table S2 of Supporting Information), i.e., a preferential hydrogen atom loss from the *methyl* group. Note that the formation of **p2**/**p2′**, which are accessible from **i9** to **i11**, can rationalize an atomic hydrogen elimination from the former *vinyl* group.

On the singlet surface, the atomic hydrogen loss from the methyl group can account for the decomposition of intermediates **s7** (**p4**), **s6** (**p2**), and **s2** and/or **s8** (**p1**), whereas the experimentally detected hydrogen loss from the vinyl group might be explained via unimolecular decomposition of **s8** to product **p2** and **s2** to product **p3**. Can we narrow down the latter pathways even further? We have to keep in mind that intermediate **s2** can decompose via atomic hydrogen loss from the methyl *and* from the vinyl group leading to **p1** and **p3**, respectively. Based on the energetics of the decomposition, **p1** (−221 kJmol^{-1}) should be formed preferentially compared to **p3** (−173 kJmol^{-1}). This conclusion gains full support from our statistical calculations indicating a preferential formation of **p1** compared to **p3** with fractions of 45% and 2%, respectively (Table 2). Therefore, intermediate **s2** loses a hydrogen atom preferentially from the *methyl* group yielding **p1**; note that **s2** can also isomerize to **s8**, which also decomposes to **p1** via hydrogen atom loss from the methyl group or to **p2** via hydrogen loss from the vinyl group. How about other pathways to the alternative reaction products **p2** and **p4**? Product **p4** can be formed via unimolecular decomposition of **s7**, with the latter being formed by isomerization of **s1**. This process, however, involves a significant barrier of 177 kJ mol^{-1} for **s1** to **s7**. Considering **s1**, our calculations identify a lower barrier of only 60 kJ mol^{-1} for the isomerization of **s1** to **s2**. Therefore, we can conclude that **s1** isomerizes preferentially to **s2** rather than to **s7**. Once again, our statistical calculations confirm this conclusion and suggest that about 99% of **s1** isomerize to **s2**. Since the formation of **s7** is of minor importance, we can predict that product **p4**, if present at all, is formed at lower fractions at most compared to **p1**. On the other hand, the energetically more stable product **p2** could be the result of a unimolecular decomposition of **s8** and **s6**, with the latter being formed from **s3** and **s5**. Since **s3** can isomerize to **s5** via a barrier of only 1 kJmol^{-1}, and **s3** connects to intermediate **s2**, we can propose that the isomerization sequence **s2** → **s3** → **s5** → **s6** might be involved in the formation of **p2** via hydrogen loss from the *methyl* group along with the **s2** → **s8** path via hydrogen loss from the *vinyl* group.

On the basis of these considerations, we would like to propose the following reaction mechanisms. On the triplet surface, the reaction involves indirect scattering dynamics and is initiated by the addition of the dicarbon reactant to the carbon−carbon double bond of propene at the C1 and/or C2 carbon atom leading to **i1** and/or **i2**. These intermediates isomerize to **i7** involving cyclization/ring-opening/ring closure pathways via two reaction sequences: (i) **i4** → **i7** (ii) **i3** → **i5** → **i6** → **i7**. Ultimately, intermediate **i7** decomposes via hydrogen atom emission from the *methyl* group through a tight exit transition state ranging 17 kJ mol^{-1} above the separated products to form product **p1**. Recall that the existence of a tight transition state was predicted based on the center-of-mass translational energy distribution. Further, the reversed addition of a hydrogen atom to an sp^2 hybridized carbon atom is expected to occur perpendicularly to the molecular plane of **p1** due to maximum orbital overlap. Therefore, this finding can also rationalize the experimentally observed sideway scattering and hence distribution maximum of the center-of-mass angular distribution at 90°. Besides the hydrogen atom loss from the methyl group leading to **p1**, the studies also identified a second channel via hydrogen elimination from the former methyl group forming **p2**/**p2′**. Here, intermediate **i2** isomerizes to **i8**. This reaction intermediate is involved in three reaction sequences: (i) **i8** → **i9** → **p2′**, (ii) **i8** → **i10** → **p2**, (iii) **i8** → **i11** → **p2′** . All exit transition states are tight. In summary, our studies suggest the formation of two isomers, **p1** and **p2**/**p2′**, on the triplet surface via hydrogen atom elimination from the *methyl* and *vinyl* group, respectively, with computed branching ratios of 23% and 35%, respectively.

On the singlet surface, the reaction is also initiated by a barrier-less addition of dicarbon, but simultaneously to both carbon atoms of the carbon−carbon double bond yielding collision complex **s1**. The latter isomerizes via ring-opening to intermediate **s2**, which then decomposes through a loose exit transition state via hydrogen atom loss from the *methyl* group to form **p1**. Recall that in related reactions of dicarbon with acetylene[54,59,82] and ethylene,[53,83] the center-of-mass translational energy distribution was found to have a broad distribution maximum similar to the dicarbon−propene system as observed here. This finding was interpreted in terms of at least two reaction mechanisms, one on the triplet and a second on the singlet surfaces involving tight and loose exit transition states, respectively. Therefore, the broad distribution maximum found in the reaction of dicarbon with propene also support the presence of ground state singlet and excited state triplet dicarbon reactants. Finally, we would like to stress that products **p2** can be also formed via atomic hydrogen loss from the methyl and vinyl groups on the singlet surface via the reaction sequences **s2** → **s3** → **s5** → **s6** → **p2** and **s2** → **s8** → **p2**, respectively.

Let us now compare RRKM calculated product branching ratios for the reaction of C_2 ($X^1\Sigma_g^+/a^3\Pi_u$) with propene (Table 2) with experimental observations and the proposed mecha-

nism. At the experimental collision energy of 21 kJmol^{-1}, the most important products of the reaction in the singlet state include **p1** (45%) mostly produced from **s2**, *i*-C_4H_3 plus CH_3 (29%, also mostly from **s2**), and **p2** (12%) formed from **s8** (8%) and **s6** (4%). On the triplet surface, the branching ratios slightly depend on which initial adduct, **i1** or **i2**, is produced in the entrance channel, but, assuming equal probabilities of the formation of these adducts, the main products are **p1** (23%), *i*-C_4H_3 plus CH_3 (17%,) **p2′/p2** (35%), and **p5** (22%). Note that according to the statistical picture from the RRKM calculations, on the singlet surface, **p1** and **p2** from **s6** are produced by a hydrogen loss from a methyl group (49%), and **p2** from **s8** is formed by a vinyl hydrogen atom loss (8%). On the triplet surface, **p1** and **p5** are formed by a methyl hydrogen loss (45%), whereas **p2′/p2** are produced a vinyl hydrogen loss (35%). This means that a statistically behaving reaction on the singlet PES alone would produce the methyl hydrogen loss to the vinyl hydrogen loss ratio of 49/8−6.1, while the triplet reaction alone would produce the methyl to vinyl hydrogen loss ratio of 45/35−1.3. Finally, we would like to comment on the cyclopentadienyl radical **p5**. Experimentally, we have no conclusive evidence that this isomer is formed in the reaction. It might be synthesized with some internal energy. However, the surfaces indicate that the dynamics factors are not favorable for the formation of **p5** as compared to the production of **p1** or **p2′/p2** because the pathways to the precursors of **p5**, **s11** and **i12**, involve multiple hydrogen shifts; deviations from the statistical behavior are expected to favor mostly **p1** and *i*-C_4H_3 plus CH_3.

6. CONCLUSION

The crossed molecular beam reactions of dicarbon, $C_2(X^1\Sigma_g^+, a^3\Pi_u)$, with propene ($C_3H_6$; X^1A') and with the partially deuterated D3 counterparts (CD_3CHCH_2, CH_3CDCD_2) were conducted at a collision energy of 21 kJ mol^{-1} under single collision conditions. The experimental data were combined with ab initio calculations to reveal the underlying reaction mechanisms. Both in the triplet and singlet surfaces, the reactions were found to be indirect via complex formation. On the triplet surface, the reaction is initiated by the addition of the dicarbon reactant to the carbon−carbon double bond of propene at the C1 and/or C2 carbon atom yielding intermediates **i1** and **i2**, respectively. These intermediates undergo mainly three isomerization sequences involving key intermediates **i7** and **i8**. Intermediate **i7** fragments via hydrogen atom loss from the methyl group yielding **p1**, whereas intermediate **i8** isomerizes to **i9-i11**, which then lose hydrogen atom(s) from the vinyl group forming **p2/p2′**. Therefore, reactions on the triplet surface yield ultimately two isomers via hydrogen losses from the *methyl* and from the *vinyl* group: 1-vinylpropargyl and 3-vinylpropargyl. On the singlet surface, the reaction is also initiated by a barrier-less addition of dicarbon, but to both carbon atoms of the carbon−carbon double bond yielding collision complex **s1**. The methylbutatriene intermediate (**s2**) was identified as the central reaction intermediate leading to product **p1** via hydrogen emission from the methyl group; also, product **p2** can be accessed via multistep isomerization sequences via hydrogen elimination from the former methyl and vinyl groups of the propene reactant. In summary, the title reaction leads to the formation of at least two distinct C_5H_5 isomers, i.e., the resonantly stabilized free radicals: 1-vinylpropargyl and 3-vinylpropargyl. In combustion flames, both radicals can undergo a hydrogen atom-assisted isomerization leading ultimately to the thermodynamically most stable cyclopentadienyl isomer, which is also considered as a precursor to indene and naphthalene.[36,37,84] Alternatively, in a third body process, a subsequent reaction of 1-vinylpropargyl or 3-vinylpropargyl radicals with the propargyl radical might yield to styrene ($C_6H_5C_2H_3$) in *an entrance barrier-less* reaction. This presents a strong alternative to the formation of styrene via the bimolecular reaction of phenyl radicals with ethylene, which is affiliated with an entrance barrier of about 10 kJ mol^{-1}.[85]

■ ASSOCIATED CONTENT

Supporting Information

Complete potential energy maps of the $C_2(X^1\Sigma_g^+) + C_3H_6$ and $C_2(a^3\Pi_u) + C_3H_6$ reactions (Figures S1 and S2, respectively), optimized Cartesian coordinates, rotational constants, and vibrational frequencies of various intermediates and products involved in the reactions (Table S1), and rate constants of various unimolecular reaction steps calculated using RRKM theory at different collision energies (Table S2). This material is available free of charge via the Internet at http://pubs.acs.org.

■ AUTHOR INFORMATION

Notes

The authors declare no competing financial interest.

■ ACKNOWLEDGMENTS

This work was supported by the U.S. Department of Energy, Basic Energy Sciences (Grants No. DE-FG02-03ER15411 to R.I.K. and the University of Hawaii and DE-FG02-04ER15570 to A.M.M. at FIU).

■ REFERENCES

(1) Koyano, M.; Endo, O.; Goto, S.; Tanabe, K.; Koottatep, S.; Matsushita, H. Carcinogenic Polynuclear Aromatic Hydrocarbons in the Atmosphere in Chiang Mai, Thailand. *Jpn. J. Tox. Env. Health* **1998**, *44*, 214−225.

(2) Feng, Z. H.; Hu, W. W.; Rom, W. N.; Costa, M.; Tang, M. S. Chromium(VI) Exposure Enhances Polycyclic Aromatic Hydrocarbon-DNA Binding at the P53 Gene in Human Lung Cells. *Carcinogenesis* **2003**, *24*, 771−778.

(3) Cohn, C. A.; Lemieux, C. L.; Long, A. S.; Kystol, J.; Vogel, U.; White, P. A.; Madsen, A. M. Physical-Chemical and Microbiological Characterization, and Mutagenic Activity of Airborne PM Sampled in a Biomass-Fueled Electrical Production Facility. *Environ. Mol. Mutagen.* **2011**, *52*, 319−330.

(4) Mansurov, Z. A. Soot Formation in Combustion Processes (Review). *Combust., Explos. Shock Waves (Engl. Transl.)* **2005**, *41*, 727−744.

(5) Cherchneff, I. The Inner Wind of IRC+10216 Revisited: New Exotic Chemistry and Diagnostic for Dust Condensation in Carbon Stars. *Astron. Astrophys.* **2012**, *545*.

(6) Yang, B.; et al. An Experimental Study of the Premixed Benzene/Oxygen/Argon Flame with Tunable Synchrotron Photoionization. *Proc. Combust. Inst.* **2007**, *31*, 555−563.

(7) Kamphus, M.; Braun-Unkhoff, M.; Kohse-Hoinghaus, K. Formation of Small PAHs in Laminar Premixed Low-Pressure Propene and Cyclopentene Flames: Experiment and Modeling. *Combust. Flame* **2008**, *152*, 28−59.

(8) Li, Y. Y.; Zhang, L. D.; Tian, Z. Y.; Yuan, T.; Wang, J.; Yang, B.; Qi, F. Experimental Study of a Fuel-Rich Premixed Toluene Flame at Low Pressure. *Energy Fuels* **2009**, *23*, 1473−1485.

(9) Li, Y. Y.; Zhang, L. D.; Tian, Z. Y.; Yuan, T.; Zhang, K. W.; Yang, B.; Qi, F. Investigation of the Rich Premixed Laminar Acetylene/Oxygen/Argon Flame: Comprehensive Flame Structure and Special Concerns of Polyynes. *Proc. Combust. Inst.* **2009**, *32*, 1293−1300.

(10) Newby, J. J.; Stearns, J. A.; Liu, C. P.; Zwier, T. S. Photochemical and Discharge-Driven Pathways to Aromatic Products from 1,3-Butadiene. *J. Phys. Chem. A* **2007**, *111*, 10914−10927.
(11) Li, Y. Y.; Zhang, L. D.; Yuan, T.; Zhang, K. W.; Yang, J. Z.; Yang, B.; Qi, F.; Law, C. K. Investigation on Fuel-Rich Premixed Flames of Monocyclic Aromatic Hydrocarbons: Part I. Intermediate Identification and Mass Spectrometric Analysis. *Combust. Flame* **2010**, *157*, 143−154.
(12) Yang, B.; Osswald, P.; Li, Y. Y.; Wang, J.; Wei, L. X.; Tian, Z. Y.; Qi, F.; Kohse-Hoinghaus, K. Identification of Combustion Intermediates in Isomeric Fuel-Rich Premixed Butanol-Oxygen Flames at Low Pressure. *Combust. Flame* **2007**, *148*, 198−209.
(13) Richter, H.; Howard, J. B. Formation of Polycyclic Aromatic Hydrocarbons and Their Growth to Soot - A Review of Chemical Reaction Pathways. *Prog. Energy Combust. Sci.* **2000**, *26*, 565−608.
(14) Fahr, A.; Nayak, A. Kinetics and Products of Propargyl (C_3H_3) Radical Self- Reactions and Propargyl-Methyl Cross-Combination Reactions. *Int. J. Chem. Kinet.* **2000**, *32*, 118−124.
(15) Frenklach, M.; Wang, H. Aromatics Growth Beyond the First Ring and the Nucleation of Soot Particles. *Abstr. Pap. Am. Chem. Soc.* **1991**, *202*, 108.
(16) Frenklach, M. Reaction Mechanism of Soot Formation in Flames. *Phys. Chem. Chem. Phys.* **2002**, *4*, 2028−2037.
(17) Maricq, M. M. Size and Charge of Soot Particles in Rich Premixed Ethylene Flames. *Combust. Flame* **2004**, *137*, 340−350.
(18) Moriarty, N. W.; Frenklach, M. Ab Initio Study of Naphthalene Formation by Addition of Vinylacetylene to Phenyl. *Proc. Combust. Inst.* **2000**, *28*, 2563−2568.
(19) Richter, H.; Howard, J. B. Formation and Consumption of Single-Ring Aromatic Hydrocarbons and Their Precursors in Premixed Acetylene, Ethylene and Benzene Flames. *Phys. Chem. Chem. Phys.* **2002**, *4*, 2038−2055.
(20) Sabbah, H.; Biennier, L.; Klippenstein, S. J.; Sims, I. R.; Rowe, B. R. Exploring the Role of PAHs in the Formation of Soot: Pyrene Dimerization. *J. Phys. Chem. Lett.* **2010**, *1*, 2962−2967.
(21) Siegmann, K.; Sattler, K. Formation Mechanism for Polycyclic Aromatic Hydrocarbons in Methane Flames. *J. Chem. Phys.* **2000**, *112*, 698−709.
(22) Hansen, N.; Miller, J. A.; Klippenstein, S. J.; Westmoreland, P. R.; Kohse-Hoinghaus, K. Exploring Formation Pathways of Aromatic Compounds in Laboratory-Based Model Flames of Aliphatic Fuels. *Combust., Explos. Shock Waves (Engl. Transl.)* **2012**, *48*, 508−515.
(23) Narendrapurapu, B. S.; Simmonett, A. C.; Schaefer, H. F.; Miller, J. A.; Kippenstein, S. J. Combustion Chemistry: Important Features of the C_3H_5 Potential Energy Surface, Including Allyl Radical, Propargyl+H_2, Allene+H, and Eight Transition States. *J. Phys. Chem. A* **2011**, *115*, 14209−14214.
(24) Zhang, T.; et al. Direct Identification of Propargyl Radical in Combustion Flames by Vacuum Ultraviolet Photoionization Mass Spectrometry. *J. Chem. Phys.* **2006**, 124.
(25) Georgievskii, Y.; Miller, J. A.; Klippenstein, S. J. Association Rate Constants for Reactions between Resonance-Stabilized Radicals: C_3H_3+C_3H_3, C_3H_3+C_3H_5, and C_3H_5+C_3H_5. *Phys. Chem. Chem. Phys.* **2007**, *9*, 4259−4268.
(26) Miller, J. A.; Klippenstein, S. J.; Georgievskii, Y.; Harding, L. B.; Allen, W. D.; Simmonett, A. C. Reactions between Resonance-Stabilized Radicals: Propargyl Plus Allyl. *J. Phys. Chem. A* **2010**, *114*, 4881−4890.
(27) Zhang, T. C.; Wang, J.; Yuan, T.; Hong, X.; Zhang, L. D.; Qi, F. Pyrolysis of Methyl *tert*-Butyl Ether (MTBE). 1. Experimental Study with Molecular-Beam Mass Spectrometry and Tunable Synchrotron VUV Photoionization. *J. Phys. Chem. A* **2008**, *112*, 10487−10494.
(28) Hansen, N.; et al. Identification and Chemistry of C_4H_3 and C_4H_5 Isomers in Fuel-Rich Flames. *J. Phys. Chem. A* **2006**, *110*, 3670−3678.
(29) Hansen, N.; Klippenstein, S. J.; Miller, J. A.; Wang, J.; Cool, T. A.; Law, M. E.; Westmoreland, P. R.; Kasper, T.; Kohse-Hoinghaus, K. Identification of C_5H_x Isomers in Fuel-Rich Flames by Photoionization Mass Spectrometry and Electronic Structure Calculations. *J. Phys. Chem. A* **2006**, *110*, 4376−4388.
(30) Mebel, A. M.; Kislov, V. V. Can the C_5H_5 + C_5H_5 → $C_{10}H_{10}$ → $C_{10}H_9$ + H/$C_{10}H_8$ + H_2 Reaction Produce Naphthalene? An Ab Initio/RRKM Study. *J. Phys. Chem. A* **2009**, *113*, 9825−9833.
(31) Miller, J. A.; Pilling, M. J.; Troe, E. Unravelling Combustion Mechanisms through a Quantitative Understanding of Elementary Reactions. *Proc. Combust. Inst.* **2005**, *30*, 43−88.
(32) Miller, J. A.; Melius, C. F. Kinetic and Thermodynamic Issues in the Formation of Aromatic-Compounds in Flames of Aliphatic Fuels. *Combust. Flame* **1992**, *91*, 21−39.
(33) Brydges, S.; Reginato, N.; Cuffe, L. P.; Seward, C. M.; McGlinchey, M. J. High and Low Barriers to Haptotropic Shifts across Polycyclic Surfaces: The Relevance of Aromatic Character During the Migration Process. *C. R. Chim.* **2005**, *8*, 1497−1505.
(34) Kaiser, R. I.; Lee, H. Y.; Mebel, A. M.; Lee, Y. T. The Formation of Isomers as Potential Key Intermediates C_5H_5 to Polycyclic Aromatic Hydrocarbon-like Molecules. *Astrophys. J.* **2001**, *548*, 852−860.
(35) Yang, B.; Huang, C. Q.; Wei, L. X.; Wang, J.; Sheng, L. S.; Zhang, Y. W.; Qi, F.; Zheng, W. X.; Li, W. K. Identification of Isomeric C_5H_3 and C_5H_5 Free Radicals in Flame with Tunable Synchrotron Photoionization. *Chem. Phys. Lett.* **2006**, *423*, 321−326.
(36) Kislov, V. V.; Mebel, A. M. The Formation of Naphthalene, Azulene, and Fulvalene from Cyclic C_5 Species in Combustion: An Ab Initio/RRKM Study of 9-H-Fulvalenyl (C_5H_5-C_5H_4) Radical Rearrangements. *J. Phys. Chem. A* **2007**, *111*, 9532−9543.
(37) Kislov, V. V.; Mebel, A. M. An Ab Initio G3-Type/Statistical Theory Study of the Formation of Indene in Combustion Flames. II. The Pathways Originating from Reactions of Cyclic C_5 Species - Cyclopentadiene and Cyclopentadienyl Radicals. *J. Phys. Chem. A* **2008**, *112*, 700−716.
(38) Lu, M. M.; Mulholland, J. A. PAH Growth from the Pyrolysis of Cpd, Indene and Naphthalene Mixture. *Chemosphere* **2004**, *55*, 605−610.
(39) Marsh, N. D.; Wornat, M. J.; Scott, L. T.; Necula, A.; Lafleur, A. L.; Plummer, E. F. The Identification of Cyclopenta-Fused and Ethynyl-Substituted Polycyclic Aromatic Hydrocarbons in Benzene Droplet Combustion Products. *Polycyclic Aromat. Compd.* **1999**, *13*, 379−402.
(40) Goel, A.; Hebgen, P.; Vander Sande, J. B.; Howard, J. B. Combustion Synthesis of Fullerenes and Fullerenic Nanostructures. *Carbon* **2002**, *40*, 177−182.
(41) Silvestrini, M.; Merchan-Merchan, W.; Richter, H.; Saveliev, A.; Kennedy, L. A. Fullerene Formation in Atmospheric Pressure Opposed Flow Oxy-Flames. *Proc. Combust. Inst.* **2005**, *30*, 2545−2552.
(42) Richter, H.; Benish, T. G.; Mazyar, O. A.; Green, W. H.; Howard, J. B. Formation of Polycyclic Aromatic Hydrocarbons and Their Radicals in a Nearly Sooting Premixed Benzene Flame. *Proc. Combust. Inst.* **2000**, *28*, 2609−2618.
(43) Granata, S.; Faravelli, T.; Ranzi, E.; Olten, N.; Senkan, S. Kinetic Modeling of Counterflow Diffusion Flames of Butadiene. *Combust. Flame* **2002**, *131*, 273−284.
(44) Lindstedt, R. P.; Rizos, K. A. The Formation and Oxidation of Aromatics in Cyclopentene and Methyl-Cyclopentadiene Mixtures. *Proc. Combust. Inst.* **2002**, *29*, 2291−2298.
(45) Gu, X. B.; Kaiser, R. I. Reaction Dynamics of Phenyl Radicals in Extreme Environments: A Crossed Molecular Beam Study. *Acc. Chem. Res.* **2009**, *42*, 290−302.
(46) Hahndorf, I.; Lee, H. Y.; Mebel, A. M.; Lin, S. H.; Lee, Y. T.; Kaiser, R. I. A Combined Crossed Beam and Ab Initio Investigation on the Reaction of Carbon Species with C_4H_6 Isomers. I. The 1,3-Butadiene Molecule, $H_2CCHCHCH_2(X^1A')$. *J. Chem. Phys.* **2000**, *113*, 9622−9636.
(47) Balucani, N.; Lee, H. Y.; Mebel, A. M.; Lee, Y. T.; Kaiser, R. I. A Combined Crossed Beam and Ab Initio Investigation on the Reaction of Carbon Species with C_4H_6 Isomers. III. 1,2-Butadiene, $H_2CCCH(CH_3)$ (X^1A') - A Non-Rice-Ramsperger-Kassel-Marcus System? *J. Chem. Phys.* **2001**, *115*, 5107−5116.

(48) Huang, L. C. L.; Lee, H. Y.; Mebel, A. M.; Lin, S. H.; Lee, Y. T.; Kaiser, R. I. A Combined Crossed Beam and ab initio Investigation on the Reaction of Carbon Species with C_4H_6 Isomers. II. The Dimethylacetylene Molecule, $H_3CCCCH_3(X^1A_{1g})$. *J. Chem. Phys.* **2000**, *113*, 9637−9648.
(49) Smith, G. P.; Park, C.; Schneiderman, J.; Luque, J. C_2 Swan Band Laser-Induced Fluorescence and Chemiluminescence in Low-Pressure Hydrocarbon Flames. *Combust. Flame* **2005**, *141*, 66−77.
(50) Blanquart, G.; Pepiot-Desjardins, P.; Pitsch, H. Chemical Mechanism for High Temperature Combustion of Engine Relevant Fuels with Emphasis on Soot Precursors. *Combust. Flame* **2009**, *156*, 588−607.
(51) Yorka, S. B. Photometric Molecular Indexes in Warm Carbon Stars - NH, CN, CH, and C_2. *Astron. J.* **1983**, *88*, 1816−1824.
(52) Marcelino, N.; Cernicharo, J.; Agundez, M.; Roueff, E.; Gerin, M.; Martin-Pintado, J.; Mauersberger, R.; Thum, C. Discovery of Interstellar Propylene (CH_2CHCH_3): Missing Links in Interstellar Gas-Phase Chemistry. *Astrophys. J.* **2007**, *665*, L127−L130.
(53) Balucani, N.; Mebel, A. M.; Lee, Y. T.; Kaiser, R. I. A Combined Crossed Molecular Beam and Ab Initio Study of the Reactions $C_2(X^1\Sigma^+_g, a^3\Pi_u) + C_2H_4 \rightarrow n\text{-}C_4H_3(X^2A') + H(^2S_{1/2})$. *J. Phys. Chem. A* **2001**, *105*, 9813−9818.
(54) Kaiser, R. I.; Balucani, N.; Charkin, D. O.; Mebel, A. M. A Crossed Beam and Ab Initio Study of the $C_2(X^1\Sigma^+_g, a^3\Pi_u) + C_2H_2(X^1\Sigma^+_g)$ Reactions. *Chem. Phys. Lett.* **2003**, *382*, 112−119.
(55) Canosa, A.; Paramo, A.; Le Picard, S. D.; Sims, I. R. An Experimental Study of the Reaction Kinetics of $C_2(X^1\Sigma^+_g)$ with Hydrocarbons (CH_4, C_2H_2, C_2H_4, C_2H_6 and C_3H_8) over the Temperature Range 24−300 K: Implications for the Atmospheres of Titan and the Giant Planets. *Icarus* **2007**, *187*, 558−568.
(56) Daugey, N.; Caubet, P.; Bergeat, A.; Costes, M.; Hickson, K. M. Reaction Kinetics to Low Temperatures. Dicarbon Plus Acetylene, Methylacetylene, Allene and Propene from $77 \leq T \leq 296$ K. *Phys. Chem. Chem. Phys.* **2008**, *10*, 729−737.
(57) Guo, Y.; Gu, X.; Kawamura, E.; Kaiser, R. I. Design of a Modular and Versatile Interlock System for Ultrahigh Vacuum Machines: A Crossed Molecular Beam Setup as a Case Study. *Rev. Sci. Instrum.* **2006**, *77*, 034701/034701−034701/034709.
(58) Kaiser, R. I.; Maksyutenko, P.; Ennis, C.; Zhang, F. T.; Gu, X. B.; Krishtal, S. P.; Mebel, A. M.; Kostko, O.; Ahmed, M. Untangling the Chemical Evolution of Titan's Atmosphere and Surface-from Homogeneous to Heterogeneous Chemistry. *Faraday Discuss.* **2010**, *147*, 429−478.
(59) Gu, X. B.; Guo, Y.; Kawamura, E.; Kaiser, R. I. Characteristics and Diagnostics of an Ultrahigh Vacuum Compatible Laser Ablation Source for Crossed Molecular Beam Experiments. *J. Vac. Sci. Technol. A* **2006**, *24*, 505−511.
(60) Daly, N. R. Scintillation-Type Mass Spectrometer Ion Detector. *Rev. Sci. Instrum.* **1960**, *31*, 264−267.
(61) Vernon, M. Ph.D. Thesis, University of California, Berkeley, Berkeley, CA, 1981.
(62) Weiss, M. S. Ph.D. Thesis, University Of California, Berkeley, Berkeley, CA, 1986.
(63) Kaiser, R. I.; Goswami, M.; Maksyutenko, P.; Zhang, F.; Kim, Y. S.; Landera, A.; Mebel, A. M. A Crossed Molecular Beams and Ab Initio Study on the Formation of C_6H_3 Radicals. An Interface between Resonantly Stabilized and Aromatic Radicals. *J. Phys. Chem. A* **2011**, *115*, 10251−10258.
(64) Becke, A. D. Density-Functional Thermochemistry. III. The Role of Exact Exchange. *J. Chem. Phys.* **1993**, *98*, 5648−5652.
(65) Lee, C. T.; Yang, W. T.; Parr, R. G. Development of the Colle−Salvetti Correlation-Energy Formula into a Functional of the Electron-Density. *Phys. Rev. B* **1988**, *37*, 785−789.
(66) Pople, J. A.; Headgordon, M.; Raghavachari, K. Quadratic Configuration-Interaction - A General Technique for Determining Electron Correlation Energies. *J. Chem. Phys.* **1987**, *87*, 5968−5975.
(67) Purvis, G. D.; Bartlett, R. J. A Full Coupled-Cluster Singles and Doubles Model - The Inclusion of Disconnected Triples. *J. Chem. Phys.* **1982**, *76*, 1910−1918.
(68) Scuseria, G. E.; Schaefer, H. F. Is Coupled Cluster Singles and Doubles (CCSD) More Computationally Intensive Than Quadratic Configuration-Interaction (QCISD). *J. Chem. Phys.* **1989**, *90*, 3700−3703.
(69) Scuseria, G. E.; Janssen, C. L.; Schaefer, H. F. An Efficient Reformulation of the Closed-Shell Coupled Cluster Single and Double Excitation (CCSD) Equations. *J. Chem. Phys.* **1988**, *89*, 7382−7387.
(70) Dunning, T. H. Gaussian-Basis Sets for Use in Correlated Molecular Calculations. I. The Atoms Boron through Neon and Hydrogen. *J. Chem. Phys.* **1989**, *90*, 1007−1023.
(71) Lee, T. J.; Taylor, P. R. A Diagnostic for Determining the Quality of Single-Reference Electron Correlation Methods. *Int. J. Quantum Chem.* **1989**, 199−207.
(72) Peterson, K. A.; Dunning, T. H. Intrinsic Errors in Several Ab-Initio Methods - The Dissociation-Energy of N_2. *J. Phys. Chem.* **1995**, *99*, 3898−3901.
(73) Frisch, M. J., et al. *Gaussian 09*, revision A.1; Gaussian, Inc: Wallingford, CT, 2009.
(74) Werner, H.-J.; Knowles, P. J.; Kinizia, G.; Manby, F. R.; Schutz, M.; Celani, P.; Korona, T.; Lindh, R. *Molpro, Version 2010.1, A Package of Ab Initio Programs*, 2010.
(75) Eyring, H.; Lin, S. H.; Lin, S. M. *Basis Chemical Kinetics*. Wiley: New York, 1980.
(76) Robinson, P. J.; Holbrook, K. A. *Unimolecular Reactions*. Prentice Hall: Engelwood Cliffs, NJ, 1972.
(77) Steinfeld, J. I.; Francisco, J. S.; Hase, W. L. *Chemical Kinetics and Dynamics*, 2nd ed.; Prentice Hall: Upper Saddle River, NJ, 1999.
(78) Kaiser, R. I.; Stranges, D.; Bevsek, H. M.; Lee, Y. T.; Suits, A. G. Crossed-Beam Reaction of Carbon Atoms with Hydrocarbon Molecules. IV. Chemical Dynamics of Methylpropargyl Radical Formation, C_4H_5, from Reaction of $C(^3P_j)$ with Propylene, C_3H_6 (X^1A'). *J. Chem. Phys.* **1997**, *106*, 4945−4953.
(79) Gu, X. B.; Guo, Y.; Mebel, A. M.; Kaiser, R. I. A Crossed Beam Investigation of the Reactions of Tricarbon Molecules, C_3 ($X^1\Sigma^+_g$),with Acetylene, C_2H_2 ($X^1\Sigma^+_g$), Ethylene, C_2H_4 (X^1A_g), and Benzene, C6H6 (X^1A_{1g}). *Chem. Phys. Lett.* **2007**, *449*, 44−52.
(80) Levine, R. D. *Molecular Reaction Dynamics*; Cambridge University Press: Cambridge, UK, 2005; p 140−141.
(81) Kaiser, R. I.; Ochsenfeld, C.; HeadGordon, M.; Lee, Y. T.; Suits, A. G. A Combined Experimental and Theoretical Study on the Formation of Interstellar C_3H Isomers. *Science* **1996**, *274*, 1508−1511.
(82) Gu, X. B.; Guo, Y.; Mebel, A. M.; Kaiser, R. I. Chemical Dynamics of the Formation of the 1,3-Butadiynyl Radical (C_4H-($X^2\Sigma^+$)) and Its Isotopomers. *J. Phys. Chem. A* **2006**, *110*, 11265−11278.
(83) Mebel, A. M.; Kaiser, R. I.; Lee, Y. T. Ab Initio Mo Study of the Global Potential Energy Surface of C_4H_4 in Triplet Electronic State and the Reactions of C (^3P_j) with C_3H_4 (Allene and Propyne) and $C_2(a^3\Pi_u)$ with $C_2H_4(X^1A_{1g}^+)$. *J. Am. Chem. Soc.* **2000**, *122*, 1776−1788.
(84) McEnally, C. S.; PFefferle, L. D. The Effects of Slight Premixing on Fuel Decomposition and Hydrocarbon Growth in Benzene-Doped Methane Nonpremixed Flames. *Combust. Flame* **2002**, *129*, 305−323.
(85) Zhang, F.; Gu, X.; Guo, Y.; Kaiser, R. I. Reaction Dynamics on the Formation of Styrene: A Crossed Molecular Beam Study of the Reaction of Phenyl Radicals with Ethylene. *J. Org. Chem.* **2007**, *72*, 7597−7604.